NASA TECHNICAL MEMORANDUM

NASA TM 73726

NASA TM 73726

TWO PHASE CHOKE FLOW IN TUBES WITH VERY LARGE L/D

by R. C. Hendricks and R. J. Simoneau
Lewis Research Center
Cleveland, Ohio 44135

TECHNICAL PAPER to be presented at the
1977 Cryogenic Engineering Conference
sponsored by the National Bureau of Standards
Boulder, Colorado, August 2-5, 1977

TWO PHASE CHOKE FLOW IN TUBES WITH VERY LARGE L/D

by R. C. Hendricks and R. J. Simoneau

National Aeronautics and Space Administration
Lewis Research Center
Cleveland, Ohio 44135

ABSTRACT

Two phase and gaseous choked flow data for fluid nitrogen were obtained for a test section which was a long constant area duct of 16 200 L/D with a diverging diffuser attached to the exit. Flow rate data were taken along five isotherms (reduced temperature of 0.81, 0.96, 1.06, 1.12, and 2.34) for reduced pressures to 3. The flow rate data were mapped in the usual manner using stagnation conditions at the inlet mixing chamber upstream of the entrance length. The results are predictable by a two-phase homogeneous equilibrium choking flow model which includes wall friction. A simplified theory which in essence decouples the long tube region from the high acceleration choking region also appears to predict the data reasonably well, but about 15 percent low.

E-9279

TWO PHASE CHOKED FLOW IN TUBES WITH VERY LARGE L/D

by R. C. Hendricks and R. J. Simoneau

National Aeronautics and Space Administration
Lewis Research Center
Cleveland, Ohio 44135

INTRODUCTION

Currently, the shuttle engine turbopump is required to boost propellant pressures to 30 MPa with proposed second generation engines requiring propellants to be delivered at pressures to 50 MPa. The problem of fluid leaking past the sealing surfaces in rotating machinery is compounded with cryogenics, high pressure, large temperature gradients, very high speeds of rotation, and static seal requirements. At lower pressure and rotation speeds, self energizing pumping seals with very close clearances have been successfully employed in a variety of sealing applications (Zuk et al. [1]). These seals frequently have very large length to hydraulic diameter ratio (L/D) passages. At the proposed operating pressures, design innovations to minimize losses are required, but choked flow data and models to make such calculations are lacking. A similar problem occurs in very long cryogenic transmission lines.

E-9279

Most two phase choked flow data reported in the literature are from experimental devices with low L/D sections with little attention given to large L/D lines.

The literature has been well surveyed in references 2 to 4. In previous experiments, the authors have studied two phase choked flows in a variety of geometries [5-11] including the orifice as a limiting case. References 12 to 16 have considered short tubes; in general for $L/D < 3$ short tubes behave much like the orifice and the effects of friction may be neglected. For larger L/D the effects of friction become increasingly important in determining the limiting mass flow rate and pressure drop. The question of two phase choked flows in large L/D tubes has, to the authors knowledge, never been resolved. Toward this end, experimental two phase choked flow data for fluid nitrogen in a tube of 16 200 L/D are presented herein.

STAR Category 34

These results should have several applications including: aerospace, aeronautical and stationary engines where higher pressure components will be used to achieve higher efficiencies; high operating pressure evaporators, liquifiers and condensers associated with the cryogenic and petrochemical industries and geothermal power production pipe lines for transmission of energy/power. In addition the results should be an aid in defining the ultimate cooling capacity of a fluid in a heat exchange device; and an aid in defining the nature of metastability and reasonable boundaries for metastable operation.

DESCRIPTION OF THE APPARATUS AND PROCEDURE

The flow system (fig. 1) is essentially that of reference 17 but modified for the present test. The test section was a coil which normally served as a heat shield for other test sections. By a fairly easy rearrangement of the plumbing the flow could be diverted through the coil.

The 16 200 L/D test apparatus was made by winding a coil of 54 turns of 0.64 cm (0.25 in.) o.d. by 0.48 cm (0.19 in.) i.d. copper tubing on a 45.7 cm (18 in.) diameter drum, yielding a 78.3 meter tube length. Coil spacing is maintained at 0.64 cm by three bakelite strips which also support the coil. The exterior of the coil was covered with $1\frac{1}{4}$ cm of multilayer insulation and as shown in figure 1, the entire apparatus was located in an evacuated environment.

The pressure taps were fabricated from 0.32 cm (1/8 in.) diameter tubing silver soldered to the tube along the inner surface of the coil at 10 coil intervals except for the last tap. The axial distance between static pressure measurements are given in Table I in terms of L/D with the first location on the tube taken as zero.

In the manner suggested by the work of Henry [18] two diffusers were fabricated and attached to the end of the long tube, one with a 7° half angle divergence section and the other a $3\frac{1}{2}^{\circ}$ half angle divergence section, see figure 2. It has been observed [18] that exit pressure measurement can be made more accurately if the exit is not abrupt. To access the effect of static tap diameter on the flow, two static taps were placed in the 7° half angle diffuser; a 0.04 cm (1/64 in.) diameter hole was

located 0.64 cm ($\frac{1}{4}$ in.) from the divergence plane and a 0.08 cm (1/16 in.) diameter hole located at 0.32 cm (1/8 in.) from the divergence plane. No adverse effects due to the pressure taps were noted. The exit pressure tap, e in Table I, was less than 1 diameter from the divergence plane.

A static pressure was measured approximately 8 tube diameters downstream from the choking plane in the 1.6 cm diameter transition tube at the exit of the diffuser leading to the back pressure control valve. This was designated back pressure.

Fluid temperatures were monitored at four positions with the following instruments: platinum thermometer in the mixing chamber, in the line open ball thermocouples at approximately 75 L/D from the mixing chamber (inlet), and approximately 50 L/D from the nozzle (outlet) and an open ball thermocouple located in a well in the diffuser body.

The tank was filled with liquid nitrogen and pressurized. The normal exhaust valve was closed in order to divert the flow into the coil. The flow control valve was wide open, and the back pressure valve was opened; the flow rate through the coil was measured at the venturi and the orifice. Adjustments of the back pressure valve caused changes in the static pressure within the transition tube without changes in the exit plane pressure or pressure profile which assured that the coil was choked.

The inlet temperature to the coil could be increased using the joule heated tube (central test apparatus) which served as a preheater for these tests.

ANALYSIS

Consider a tube of length L and diameter D:

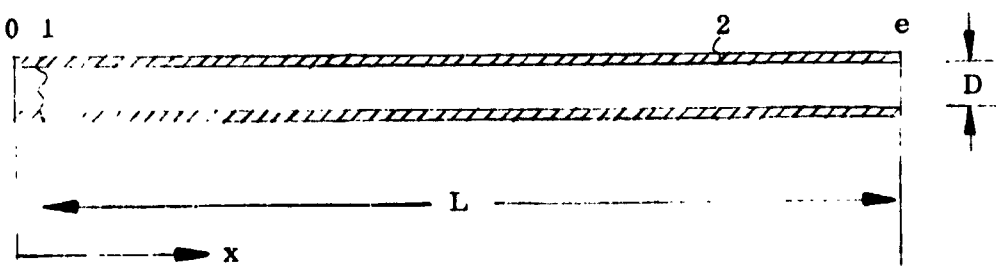

The tube has potentially three flow regions:

Entrance (0-1): Since we are dealing with a single phase incompressible, or nearly incompressible, fluid at the entrance, we can simply assign a standard head loss for the entrance configuration. Then using the friction factor we can extend the tube length appropriately.

Single phase (1-2): This region is normally dominated by friction but as the fluid gets closer to the thermodynamic critical point the flow will become more compressible. In some cases points 2 and e will coincide.

Two-phase (2-e): This region is normally dominated by the momentum of the expanding two-phase fluid, however, if vaporization occurs early enough in a long tube, wall friction may also be important in this region.

The basic equation for one-dimensional flow with friction can be written

$$\frac{dP}{fv} + G^2 \frac{dv}{fv} + \frac{G^2}{2D} dz = 0 \tag{1}$$

where

$$v = \begin{cases} v(P) & P \geq P_{sat} \\ v_m(P) = \left[\frac{kx + (1 - x)}{k}\right] \left[xv_g + (1 - x)kv_\ell\right] & P < P_{sat} \end{cases} \tag{2}$$

for a given path (e.g., isenthalpic)

$$f = f(Re) = f\left(\frac{GD}{\mu}\right) = f(P) \tag{3}$$

The friction factor f is the standard Fanning friction factor and is computed based on Reynolds number for a smooth tube. Since G is constant the friction factor is dependent only on the fluid viscosity and thus becomes a thermodynamic variable. In the two-phase region the question becomes one of what fluid is in contact with the wall. At least initially it is expected that there will be a vapor annulus and liquid core [3]. Later the flow becomes thoroughly dispersed and the overwhelming majority of the wall area will be in contact with vapor. Thus in this

analysis the two-phase wall friction factor will be based on the vapor viscosity.

The flow is assumed to be homogeneous (k = 1) and in thermodynamic equilibrium. Reference 3 suggests that this assumption becomes more valid as tube length increases, which is the case herein. The thermodynamic path is assumed to be isenthalpic. Since G is constant, equation (1) can be integrated and rearranged in the form

$$G^2 = -\frac{\int_{P_0}^{P} \frac{1}{fv}\, dv}{\int_{P_0}^{P} \frac{1}{fv}\frac{dv}{dP}\, dP + \frac{z}{2D}} \tag{4}$$

To determine choking, the derivative dG/dP is examined at the exit plane. Differentiating equation (4) yields

$$2G\frac{dG}{dP}\int_{P_0}^{P} \frac{1}{fv}\frac{dv}{dP}\, dP + \frac{z}{2D} = -G^2\left(\frac{1}{fv}\frac{dv}{dP} + \frac{1}{2D}\frac{dz}{dP}\right) - \left(\frac{1}{fv}\right) \tag{5}$$

The choking condition requires $dG/dP)_e = 0$. Thus

$$G_{max}^2 = \frac{-1}{\frac{dv}{dP} + \frac{fv}{2D}\frac{dz}{dP}}_{e} \tag{6}$$

It is known that at the exit plane dP/dz becomes very large, approaching infinity in the ideal case. Thus at the exit dz/dP can be neglected relative to dv/dP with the familiar result

$$G_{max}^2 = \left(\frac{dv}{dP}\right)_e^{-1} \tag{7}$$

By substituting L' for z in equation (4) and iterating between equations (4) and (7) the exit pressure, P_e, and the choked maximum flow rate, G_{max}, can be obtained. While in the present report the point of vaporization is taken as the equilibrium

saturation pressure, a nonequilibrium vaporization point could be defined.

Once the maximum mass flux is determined, equation (4) can be used to solve for the pressure distribution along the tube.

Special Case

In many cases, especially in very long tubes and when the initial conditions are well away from saturation, some simplifying assumptions can be applied, which allow simple estimates of the maximum flow rates.

1. The two-phase region, dominated by momentum, is very short and friction can be neglected.

2. The single-phase region, dominated by friction, is very long and relatively incompressible. Thus specific volume and friction factor can be taken as constant and the length L_{0-2} can be taken as L'.

Thus equation (4) can be simplified to

$$G_{max}^2 \approx \frac{2(P_0 - P_{sat})}{\bar{v} f (L'/D)} \tag{8}$$

Clearly equation (8) is the standard single phase friction flow equation found in any fluid mechanics text and it is not necessary to use the above analysis to arrive at it. It is recommended herein that the proper approach is the simultaneous solution of equations (4) and (7) with real fluid properties, such as available in reference 19. On the other hand it is reassuring that equations (4) and (7) reduce to a well-known form and that equation (8) can be used to compute flow rate in a fair number of cases. The exercise in obtaining the simplification also shows regimes where it might be applicable.

RESULTS

Data for fluid nitrogen were acquired and are presented in Table II. The five isotherms are presented as figure 3. In figure 3, the mass flux G and the reduced mass flux ($G_r = G/G^*$) are given as a function of reduced pressure $P_r = P_0/P_c$ where P_0 is the pressure measured at the mixing chamber. The five isotherms (0.81, 0.96, 1.06, 1.12, and 2.34) are also based on the mixing chamber tempera-

ture $T_r = T_0/T_c$. The data appear to be repre ented quite well using these mixing chamber parameters even though the choked interface is over 16 200 L/D from the mixing chamber.

The mass flux-pressure map of figure 3 resembles the shape and trends of the same map for a nozzle without an entry length at the same reduced pressure; however, the value of $G_{max, r}$ is approximately 0. 1 that for the nozzle without the 16 200 L/D entry section.

The analysis tends to underpredict the flow at the high pressure end by about 12 percent, while at the lower pressures the data and analysis are quite close. The program was designed for computing isenthalpic below the critical enthalpy; however, some of the data at higher temperatures and lower pressures are above critical enthalpy, thus only a partial check can be made. The difference in the trend is somewhat disturbing. It could be in the data. The data plotted were metered with the orifice downstream of the test section. The upstream venturi was about 8 percent lower at high pressure but at low pressure was unreliable. Since the orifice showed a consistent trend throughout the authors stuck with it. It should be pointed out, however, that in these long tubes the flows were about one-tenth the normal flow for the test rig and thus the usual high level of flow accuracy was not present. It also should be pointed out that even though there exists a 10 to 15 percent discrepancy in measured versus calculated flow the one-dimensional homogeneous equilibrium analysis with friction is closely predicting flows that are an order of magnitude below nozzle flows.

Such a reduction is borne out by the pressure - L/D profiles of figure 4, where the pressure at 100 L/D ahead of the nozzle is approximately 0. 1 P_0. For the sake of clarity only six profiles were plotted; however, these are typical of the data presented in figure 3. They are tabulated in Table III. Curiously the analysis does an excellent job of predicting the pressure profiles over the whole range of the experiment.

Another interesting trend appears in the slope of the pressure profiles depending on whether or not T_0 is above or below T_c, (T_c = 126.3 K). Such is associated with the friction-momentum pressure losses in the coil as $T_r \approx 1$. Actually a closer examination shows the profiles tend to become more curved as $H_0 \rightarrow H_c$. All of the data are for $H_0 < H_c$, however, the two dashed curves are for H_0 very close to H_c. The calculated curve for T_0 = 141.9 K actually crosses all the other curves and so do the data. At low temperature (and low enthalpy) the calculated profiles are linear in the single phase region, however, the data show a slight concave curvature.

Figure 5 is a plot of the simple equation (8). The more exact analysis is superimposed. As can be seen the equation of simple single phase friction does a good job, although it underpredicts further. It can be used with confidence for quick calculations. Not too surprisingly, the simple friction approach is best at low temperature where the fluid is highly incompressible and the saturation pressure is low.

SUMMARY

Two phase choked flow data for fluid nitrogen flowing through a 16 2000 L/D coil were taken along five isotherms (0.81, 0.96, 1.06, 1.12, and 2.34). These data can be represented by the same parameters associated with two phase choked flows without a large entry length.

Theoretical calculations indicate that a homogeneous equilibrium model, representing an integral of friction and momentum predicts the flow data with reasonable accuracy and the pressure profiles quite well. A simple equation based on the friction pressure drop in the single phase region also predicts the flow quite well.

NOTATION

D diameter, cm

f friction factor (Darcy)

G flow rate, g/cm^2-s

G^* flow normalizing parameter (6010 g/cm^2-s for nitrogen), $\sqrt{\rho_c P_c / Z_c}$

H enthalpy, J/g-K

k two-phase slip ratio, u_g/u_ℓ

L	length, cm
L'	length, including adjustment for entrance losses, cm
P	pressure, MPa
R	gas constant, MPa cm^3/g-K
Re	Reynolds number, GD/μ
T	temperature, K
U	velocity, cm/s
v	specific volume, cm^3/g
x	quality
Z	compressibility, $P/\rho RT$
z	axial distance along tube, cm
μ	viscosity, g/cm-s
ρ	density, g/cm^3

Subscripts

c	thermodynamic critical point
e	tube exit
g	saturated gas (vapor)
ℓ	saturated liquid
max	maximum value
r	reduced by corresponding states parameter
sat	saturation value
0	stagnation (tube entrance)
1	point on the tube
2	point of two phase in the tube

Superscripts

*	reference condition
$\bar{}$	average value

REFERENCES

1. J. Zuk, NASA TN D-8151 (1976).
2. Y. Y. Hsu, NASA TN D-6814 (1972).
3. R. E. Henry, M. A. Grolmes, and H. K. Fauske, Heat Transfer at Low Temperatures, W. Frost, ed., Plenum Press, New York (1975), p. 229.
4. R. V. Smith, NBS Tech Note 633 (1973).
5. R. C. Hendricks, R. J. Simoneau, and R. C. Ehlers, in Advances in Cryogenic Engineering, Vol. 18, K. D. Timmerhaus, ed., Plenum Press, New York (1973), p. 150.
6. R. C. Hendricks, R. J. Simoneau, and Y. Y. Hsu, in Advances in Cryogenic Engineering, Vol. 20, K. D. Timmerhaus, ed., Plenum Press, New York (1975), p. 370.
7. R. J. Simoneau, in Proceedings of the Tenth Southeastern Seminar on Thermal Sciences, F. G. Watts and H. H. Sogin, eds., Tulane Univ. (1974), p. 225.
8. R. J. Simoneau, in Advances in Cryogenic Engineering, Vol. 21, E. D. Timmerhaus and D. H. Weitzel, Plenum Press, New York (1975), p. 299.
9. R. C. Hendricks, R. J. Simoneau, and R. F. Barrows, NASA TN D-8169 (1976).
10. R. J. Simoneau, "Pressure Distribution in a Converging-Diverging Nozzle During Two-Phase Choked Flow of Subcooled Nitrogen," presented at the Winter Annual Meeting of the American Society of Mechanical Engineers, Houston, Texas (Nov. 30-Dec. 5, 1975).
11. R. C. Hendricks, in Proceedings of Fifth International Cryogenic Engineering Conference, K. Mendelssohn, ed., IPC Business Press, Ltd., London (1974), p. 278.
12. R. J. Richards, R. B. Jacobs, and W. J. Pestalozzi, in Advances in Cryogenic Engineering, Vol. 4, K. D. Timmerhaus, ed., Plenum Press, New York (1960), p. 272.
13. J. A. Brennan, in Advances in Cryogenic Engineering, Vol. 9, K. D. Timmerhaus, ed., Plenum Press, New York (1964), p. 292.
14. J. C. Hesson and R. E. Peck, Am. Inst. Chem. Eng. J., 4:207 (1958)
15. F. W. Bonnet, in Advances in Cryogenic Engineering, Vol. 12, K. K. Timmerhaus, ed., Plenum Press, New York (1967), p. 427.

16. H. Uchida and H. Nariai, Proceedings of the Third International Heat Transfer Conference, Vol. 5, Am. Inst. Chem. Engrs., New York (1966), p. 1.

17. R. C. Hendricks, et al., NASA TN D-3095 (1966).

18. R. E. Henry, Argonne Nat. Lab. Rept. 7430 (1968).

19. R. C. Hendricks, A. K. Baron, and I. C. Peller, NASA TN D-7808 (1975).

Table I. Pressure Tap Spacing in Terms of L/D

Station	Mix	1	2	3	4	5	6	7	e	Back
L/D	-125	0	3000	6000	9000	12 000	15 000	16 100	16 200	16 208

Table II. Data Summary

(a) $T_r = 0.81$

Run	T_{mix}, K	P_{mix}, MPa	Tube temperatures, K			Tube pressures, MPa								P_{back}, MPa	G, g/cm^2-s
			Line in	Line out	Well	1	2	3	4	5	6	7	e		
338	[a]102	10.06	104	101	99	9.68	8.04	6.35	4.63	2.96	1.42	0.85	0.36	0.34	901
340	↓	8.09	104	100	94	7.78	6.47	5.13	3.76	2.45	1.23	.77	.31	.31	800
341		7.08	104	99	93	6.81	5.69	4.51	3.33	2.20	1.14	.74	.29	.30	742
342		6.17	105	98	93	5.92	4.96	3.96	2.95	1.98	1.08	.70	.27	.28	697
343		5.05	105	97	92	4.86	4.10	3.29	2.49	1.72	.99	.66	.24	.26	594
344		4.37	106	96	91	4.21	3.57	2.89	2.21	1.56	.96	.62	.22	.25	522
345		3.39	107	95	90	3.27	2.81	2.31	1.82	1.35	.92	.56	.19	.22	408
346		2.79	106	93	89	2.68	2.32	1.93	1.55	1.18	.84	.50	.18	.21	369
347		2.24	105	92	89	2.16	1.90	1.60	1.32	1.04	.77	.44	.17	.19	293
348		1.82	105	90	89	1.75	1.58	1.36	1.16	.96	.71	.39	.16	.18	275
349		1.55	106	89	88	----	1.38	1.21	1.07	.92	.66	.35	.15	.16	207
350		1.32	111	93	89	1.25	1.10	.89	.69	.50	.28	.18	.13	.14	112
351	↓	1.09	108	91	89	1.04	.97	.81	.65	.46	.28	.17	.13	.14	99

[a]102±1 K was assigned after selected reruns were made which reproduced tube temperatures, flow rate, tank temperature, and pressure profile data.

Table II. Continued.

(b) $T_r = 0.96$

Run	T_{mix}, K	P_{mix}, MPa	Tube temperatures, K			Tube pressures, MPa								P_{back}, MPa	G, g/cm^2-s
			Line in	Line out	Well	1	2	3	4	5	6	7	e		
355	119	9.49	124	106	97	9.15	7.75	6.34	4.89	3.48	2.15	1.23	0.40	0.35	797
356	121	10.22	125	107	97	9.85	8.36	6.83	5.26	3.73	2.29	1.30	.42	.36	824
357	121	8.10	125	104	96	6.69	6.69	5.52	4.34	3.21	2.10	1.14	.36	.32	699
358	121	6.71	125	103	95	5.60	5.60	4.68	3.76	2.88	1.95	1.03	.31	.30	600
359	121	5.72	125	101	94	5.52	4.83	4.09	3.36	2.65	1.81	.93	.27	.27	518
360	120.5	4.81	125	100	93	4.64	4.12	3.54	2.97	2.43	1.65	.83	.24	.25	437
361	121	3.92	125	97	91	3.79	3.43	3.02	2.63	2.21	1.45	.71	.19	.22	349
362	121	3.15	125	95	90	3.06	2.85	2.59	2.32	1.91	1.22	.57	.15	.19	265
363	121	2.66	125	91	87	2.59	2.19	2.19	1.91	1.54	.93	.41	.12	.16	175

Table II. Continued.

(c) $T_r = 1.06$

Run	T_{mix}, K	P_{mix}, MPa	Tube temperatures, K			Tube pressures, MPa								P_{back}, MPa	G, g/cm^2-s
			Line in	Line out	Well	1	2	3	4	5	6	7	e		
365	133.5	9.89	137	107	97	9.56	8.25	6.92	5.52	4.14	2.68	1.38	0.43	0.36	715
366	134	8.69	138	106	97	8.39	7.32	6.18	5.01	3.85	2.51	1.27	.39	.33	633
367	134	7.16	138	104	96	7.21	6.34	5.43	4.49	3.54	2.30	1.14	.34	.30	557
368	134	6.16	138	102	94	5.96	5.32	4.63	3.92	3.19	2.02	.99	.28	.27	449
369	134	4.92	137	99	91	4.76	4.33	3.83	3.31	2.70	1.67	.81	.22	.22	326
370	133	4.12	137	97	88	3.98	3.61	3.16	2.67	2.12	1.31	.63	.17	.18	230
371	133	3.74	136	96	89	3.61	3.28	2.85	2.38	1.83	1.08	.54	.15	.17	195
372	133	2.96	136	107	102	2.85	2.60	2.25	1.89	1.44	.83	.40	.11	.15	138
373	135	2.75	138	107	99	2.64	2.40	2.08	1.74	1.32	.76	.36	.10	.14	129
374	134	2.21	138	115	108	2.13	1.94	1.68	1.41	1.07	.61	.29	.08	.14	99
375	134	1.77	137	115	121	1.69	1.54	1.32	1.10	.83	.48	.23	.08	.13	75
376	133	1.30	136	130	128	1.25	1.15	.99	.85	.66	.38	.18	.11	.13	51

Table II. Continued.

(d) T_r = 1.12

Run	T_{mix}, K	P_{mix}, MPa	Tube temperatures, K			Tube pressures, MPa								P_{back}, MPa	G, g/cm^2-s
			Line in	Line out	Well	1	2	3	4	5	6	7	e		
377	142	10.10	146	108	99	9.72	8.47	7.18	5.78	4.36	2.77	1.41	0.43	0.29	674
378	142	8.89	146	106	97	8.58	7.55	6.43	5.24	3.94	2.56	1.28	.39	.33	595
379	142	7.65	146	105	96	7.39	6.55	5.63	4.65	3.61	2.28	1.14	.34	.29	502
380	142	6.24	146	102	93	6.03	5.39	4.67	3.89	3.01	1.90	.94	.27	.25	382
381	142	5.23	146	99	90	5.05	4.55	3.95	3.28	2.50	1.51	.76	.21	.20	287
382	142	4.50	146	101	94	4.36	3.93	3.41	2.84	2.17	1.25	.61	.18	.18	230
384	142	3.94	146	108	100	3.81	3.45	3.00	2.50	1.90	1.10	.52	.15	.16	190
385	143	3.40	146	116	108	3.29	2.99	2.59	2.17	1.65	.95	.45	.13	.15	155
386	142	3.37	145	116	113	3.25	2.96	2.57	2.15	1.64	.94	.45	.13	.15	153
387	144	2.44	148	126	111	2.35	2.14	1.85	1.56	1.18	.68	.32	.09	.13	104
388	143	1.81	146	126	128	1.74	1.59	1.37	1.14	.87	.49	.23	.06	.13	76

Table II. Concluded.

(e) $T_r = 2.34$

Run	T_{mix}, K	P_{mix}, MPa	Tube temperatures, K			Tube pressures, MPa								P_{back}, MPa	G, g/cm^2-s
			Line in	Line out	Well	1	2	3	4	5	6	7	e		
328	296	10.1	295	272	268	9.87	8.87	7.78	6.45	4.91	2.80	1.31	0.37	0.26	282
329	295	10.1	294	274	270	9.87	8.88	7.78	6.46	4.92	2.81	1.32	.37	.44	284
330	296	8.89	295	275	270	8.67	7.81	6.84	5.68	4.32	2.47	1.15	.32	.23	246
331	296	7.55	295	277	271	7.36	6.65	5.81	4.83	3.68	2.10	.97	.27	.21	207
332	296	6.17	295	279	273	6.00	5.43	4.74	3.91	3.00	1.71	.79	.22	.18	166
333	296	4.97	295	281	275	4.84	4.39	3.83	3.19	2.43	1.39	.64	.18	.16	136
334	295	3.69	295	282	278	3.59	3.25	2.84	2.36	1.80	1.02	.47	.12	.18	98
335	296	2.35	295	285	282	2.27	2.07	1.79	1.50	1.14	.64	.29	.08	.14	61
336	295	1.52	295	286	284	1.46	1.34	1.15	.97	.73	.42	.19	.10	.12	41
337	295	1.42	295	287	286	1.36	1.25	1.08	.90	.68	.39	.19	.11	.13	43

Table III. Selected Pressure Profiles

Run	246	250	269	261	256	280
T_0, K	101.5	102.2	116.6	128.4	130.2	141.9
P_{mix}, MPa	9.77	4.65	9.78	3.87	10.05	9.70
P_1, MPa	9.43	4.50	9.43	3.79	9.74	9.38
P_2, MPa	7.85	3.83	8.01	3.52	8.37	8.23
P_3, MPa	6.23	3.10	6.63	3.19	6.96	7.09
P_4, MPa	4.59	2.39	5.03	2.81	5.51	5.70
P_5, MPa	2.99	1.70	3.49	2.25	4.07	4.27
P_6, MPa	1.50	1.07	2.09	1.39	2.63	2.73
P_7, MPa	0.92	0.67	1.22	0.66	1.38	1.37
P_e, MPa	0.37	0.23	0.40	0.18	0.44	0.44
P_{back}, MPa	0.34	0.25	0.35	0.19	0.36	0.34
G, g/cm^2-s	835	502	775	260	720	6.0

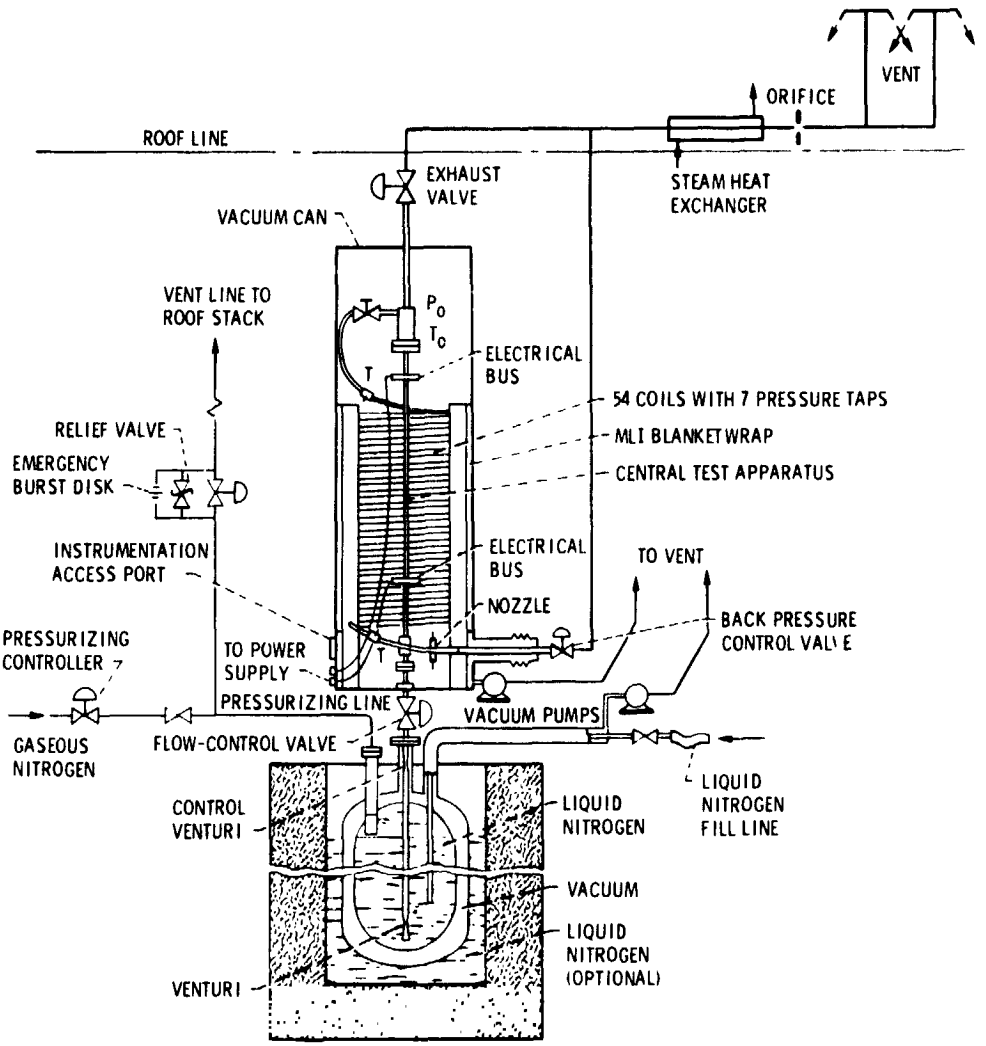

Figure 1. - Schematic of test installation.

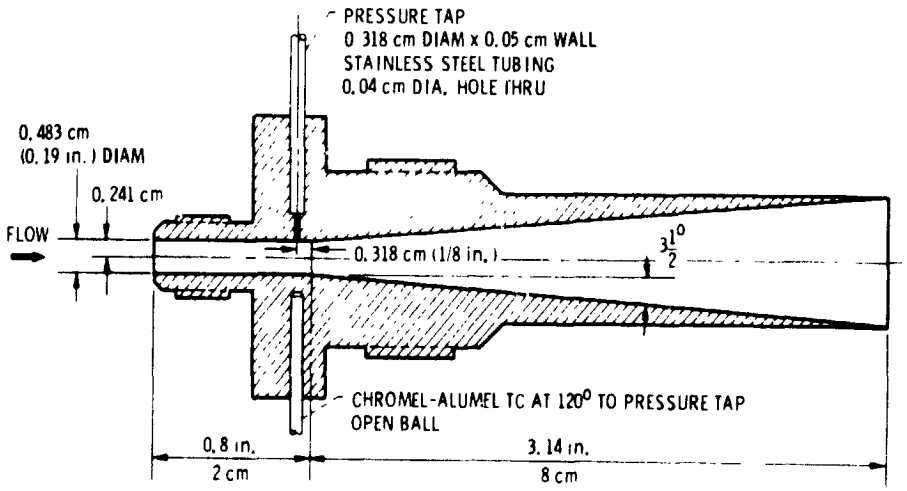

Figure 2. - Exit diffuser for 16 200 L/D test coil

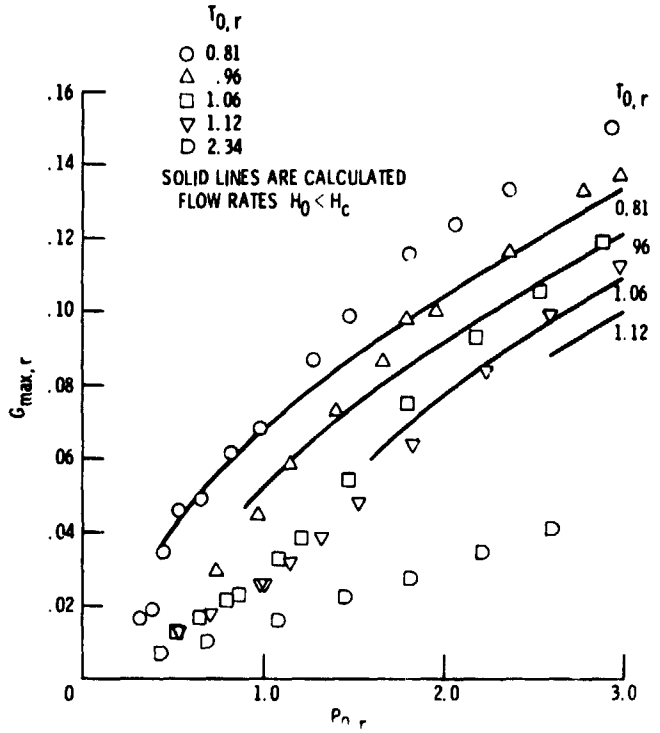

Figure 3. - Experimental and calculated reduced flow rate versus reduced pressure for 16 200 L/D test coil.

CS-77-1183

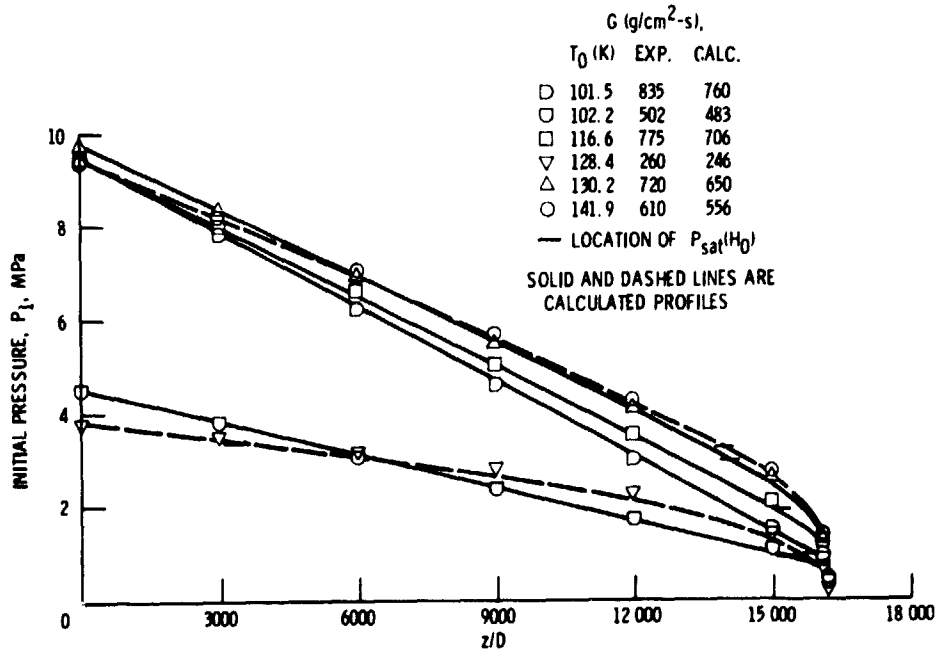

CS-77-1184

Figure 4 - Experimental and calculated axial pressure profiles for the 16 200 L/D test coil.

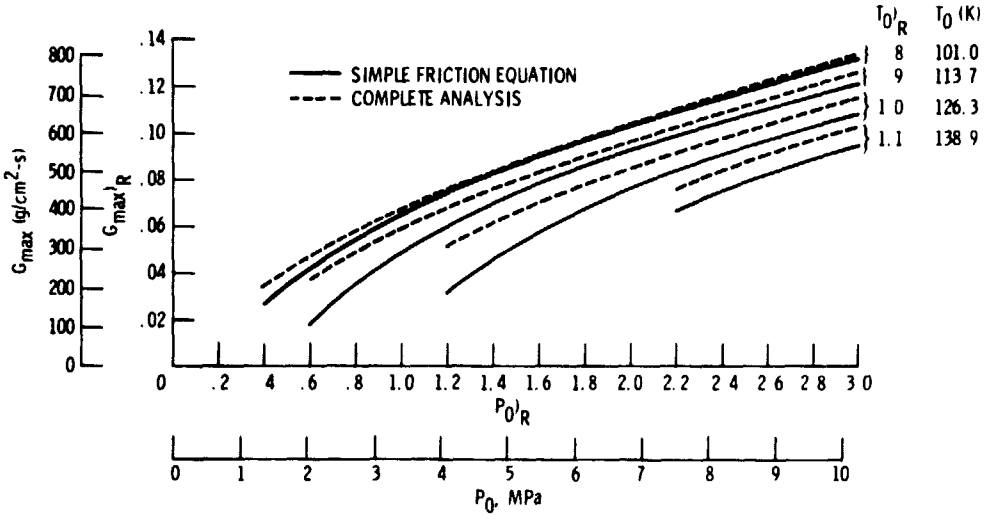

Figure 5. - Approximate computation of maximum flow rate in long tubes with phase change at the exit - equation (12). (Isenthalpic path; $H_0 < H_c$)